Predictive Control Framework for Thermal Management of Automotive Fuel Cell Systems at High Ambient Temperatures

Pier Giuseppe Anselma, Sara Luciani, Andrea Tonoli

Department of Mechanical and Aerospace Engineering (DIMEAS), Politecnico di Torino, 10129 Torino, Italy
(e-mail: pier.anselma@polito.it, sara.luciani@polito.it).

Center for Automotive Research and Sustainable Mobility (CARS), Politecnico di Torino, 10129 Torino, Italy

Abstract: Environmental conditions have a significant effect on the performance of fuel cell systems. This paper studies the vehicle hydrogen consumption, the thermal management system, and the thermal loads of an automotive fuel cell system. A predictive control framework for thermal management is investigated to minimize the overall hydrogen consumption. Initially, a numerical modeling approach for the automotive fuel cell system is presented from electrochemical and thermal perspectives. Then, the problem formulation related to the thermal management strategy is presented and solved with an optimization method based on dynamic programming (DP). The implemented DP exploits the a priori knowledge of the driving mission to appropriately control the fuel cell system gross power and the operation of the radiator fan, the coolant pump, and the compressor. Optimization constraints involve maintaining the fuel cell stack temperature below the operational limit and avoiding the thermal system from being activated when the vehicle is at rest. The fuel cell system is tested while the vehicle performs different numbers of repetitions of the Worldwide Harmonized Light Vehicle Test Procedure (WLTP) at high ambient temperature. Using the proposed predictive control framework for thermal management, results demonstrate that an average 62.5% to 63.0% efficiency can be attained by the fuel cell stack in extreme ambient conditions both in short distance and long distance driving missions.

Keywords: Automotive, fuel cell system, dynamic programming, predictive control, thermal management

1. INTRODUCTION

Uncertainties in fuel pricing and availability, as well as air-pollution issues, provide significant hurdles to the automotive sector, Ajanovic et al. (2019). To address these issues, several academics and car makers have started developing and enhancing pure electric vehicles and fuel cell electric vehicles (FCEV). FCEVs are especially promising since they are eco-friendly and achieve long driving ranges, rapid refilling capabilities, and high energy efficiency, Bethoux (2020). The temperature of a fuel cell system is a significant performance changing factor since it affects the fuel cell stack humidity, power production capability, voltage, leakage current, catalyst tolerance and durability, Salam et al. (2020). For this reason, a proper thermal management system is required to guarantee efficiency and temperature stability of the fuel cell while optimising the overall power consumption of the auxiliaries.

Many control techniques for thermal management of fuel cell systems in the literature are of reactive type. They mainly focus on the operating stack temperature without considering the efficiency of the auxiliary systems in the thermal loop. Because of their reliability and low cost, on/off switching controllers and PID (proportional integral derivative) controllers have been extensively employed in many automotive thermal control applications, Liu et al. (2011). For instance, Ibrahim et al. (2012) proposed a fuzzy-based

temperature controller for cabin heating in electric vehicles. The control was able to maintain the target temperature under different initial conditions. On the other hand, Binrui et al. (2009) proposed a fuzzy incremental PID approach to control the temperature of a proton exchange membrane (PEM) fuel cell. A self-learning intelligent control technique for ensuring cabin thermal comfort was presented by Xie et al. (2020) while Han et al. (2017) investigated different control algorithms to adapt the PEM fuel cell stack temperature to the reference value in transient conditions.

As opposed to reactive controllers, predictive thermal management approaches are emerging. They exploit the prediction of future operating conditions (e.g. utilizing traffic or road information) to reduce hydrogen consumption of FCEVs and improve fuel cell stack efficiency. For example, Han et al. (2017) recently proposed a feedback controller including model reference adaptive control to control the coolant inlet temperature. Moreover, a model predictive control (MPC) approach has been proposed to control the blowers in the fuel cell system by Zhang et al. (2020). Nevertheless, the developed predictive controller was not benchmarked with the respective global optimal solution and only some components of the thermal loop were considered in the analysis. Indeed, a systematic approach to assess the potential of predictive thermal management for FCEVs in terms of optimal fuel cell stack operation points still requires
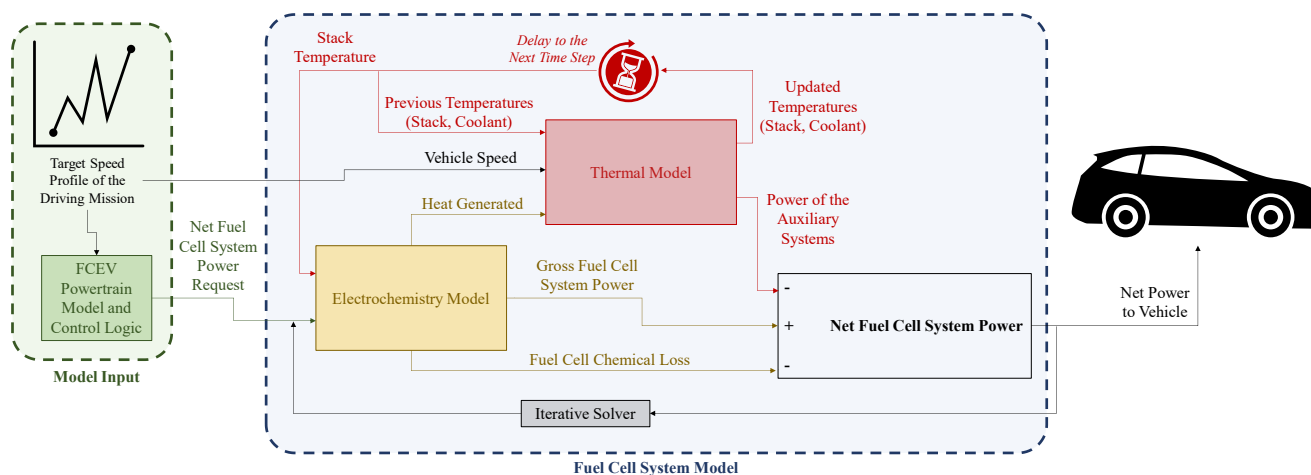
Fig. 1. Workflow of the numerical model for the fuel cell system from both electrochemical and thermal points of view.

extensive development in the cited literature. This especially holds when considering critical vehicle use cases such as when high ambient temperatures are encountered for example.

To contribute filling the identified research gap, this paper aims at developing a predictive control framework for thermal management of automotive fuel cell system with two main objectives:

1) Control the radiator fan state, the coolant mass flow rate and air mass flow rate of the fuel cell system to improve hydrogen economy at high ambient temperatures.

2) Provide a global optimal thermal management reference for the development of real-time predictive control strategies.

The paper is organized as follows. Section 2 presents the fuel cell electrochemical and thermal models under study. A global optimal predictive thermal management approach based on dynamic programming (DP) is introduced in section 3. The potential of the implemented predictive thermal management as a hydrogen saving enabler is then evaluated in section 4 by simulating the FCEV in driving missions at high ambient temperatures distinguished by different driving distances. Finally, conclusions are given in section 5.

2. THERMAL MODELLING OF AUTOMOTIVE FUEL CELL SYSTEMS

This section describes the numerical model of the automotive fuel cell system both from electrochemical and thermal points of view. In this work, the numerical method used to model the fuel cell system is semi-empirical and considers also its transient behaviour. It has been developed by Virginia Tech in collaboration with National Renewable Energy Laboratory (NREL) and implemented in the Advisor™ 2003 simulation tool embedded in Matlab® software, Gurski (2002). Fig. 1 shows the workflow of the numerical model implemented in this work to analyze the electrochemical and thermal behaviors of the automotive fuel cell system. Here, all the described numerical models are implemented in MATLAB® software.

2.1 Model inputs

The profile of the target vehicle speed over time for the retained driving mission is considered as input. The considered FCEV is a passenger car powered by an electric motor that is linked to the wheels through a direct drive. The electric motor can be powered by both the fuel cell system and a battery pack. A vehicle supervisory control algorithm and a FCEV powertrain model are implemented. They allow managing the instantaneous electrical power split between the fuel cell system and the high-voltage battery pack. Here, the vehicle supervisory control algorithm is a rule-based thermostatic logic inherited from Advisor™ 2003, Markel et al. (2002). The vehicle speed and net fuel cell system power request ($P_{stack-request}$) are received as input by the fuel cell system model. This latter is organized in two main sub-models in Fig. 1 which represent the electrochemical and thermal phenomena.

2.2 Electrochemistry Model

The electrochemistry model allows achieving two main objectives concerning the operating conditions of the fuel cell system:

1) Determine the system electrical operating conditions in terms of voltage and current density along with the H2 mass flow rate;

2) Evaluate the heat generated by the system, which is in turn fed to the thermal model.

In this framework, to let the net electrical power generated by the fuel cell system balancing the vehicle power request, it is necessary to resort to an iterative solver. An initial guess is required for stack current density I_{stack}. Then, the cell voltage V_{cell} can be determined using the polarization equation developed by Nelson and reported in (1):

$$V_{cell}(I_{stack}, T_{stack}, p_{O2}) = OCV_{cell} - V_{tafel}(I_{stack}) - V_{ohmic}(I_{stack}, T_{stack}) - V_{concentration}(I_{stack}, p_{O2}) + V_{temperature}(I_{stack}, T_{stack}) \qquad (1)$$

where OCV_{cell} and V_{tafel} are the cell open-circuit voltage and a term related with activation voltage loss as a function of the stack current density. V_{ohmic} stands for a voltage drop term related to resistance or ohmic losses in the cell as a function of the stack current density and temperature T_{stack} in kelvin as provided by the thermal model. $V_{concentration}$ accounts for the concentration of mass transportation losses in the cell as a function of the stack current density and the oxygen partial pressure at the cathode inlet p_{O2}. Finally, $V_{temperature}$ considers the effects of the stack temperature on the cell voltage. The gross fuel cell system power $P_{stack-gross}$ in watts can then be obtained using (2):

$$P_{stack-gross} = I_{stack} \cdot OCV_{cell} \cdot A_{cell} \cdot n_{cell} \quad (2)$$

where A_{cell} and n_{cell} are the area of a single cell in centimetres square and the number of cells contained in the stack, respectively. Once the value of $P_{stack-gross}$ is known, the H2 mass flow rate $\dot{m}_{H2}$ in kilograms per second can be evaluated using (3), Larminie et al. (2003).

$$\dot{m}_{H2} = \frac{P_{stack-gross} \cdot 1.05e^{-8}}{V_{cell}} \quad (3)$$

Finally, the instantaneous heat generated by the stack (Q_{stack}) can be obtained using (4):

$$Q_{stack} = \dot{m}_{H2} \cdot LHV_{H2} - P_{stack-gross} \quad (4)$$

where LHV_{H2} stands for the hydrogen lower heating value which is assumed being 1.1968e8 J/Kg here.

2.3 Thermal Model

The fuel cell system thermal model shown in Fig. 1 involves six main components represented by the air compressor, the coolant pump, the radiator fan, and the condenser fan along with the fuel cell stack and the humidifier. In general, the thermal model receives as instantaneous input the heat generated by the fuel cell system, the vehicle longitudinal speed, and the current values of temperatures. Each component is then modelled according to energy and mass balances to enable evaluating the corresponding outlet temperatures and electrical energy consumptions.

Concerning the air compressor, empirical lookup tables are used to evaluate its adiabatic efficiency ($\eta_{adiabatic}$) and its temperature rise as a function of the air flow rate ($\dot{m}_{air}$) and the related ratio between inlet and ambient air pressures (p_{ratio}). Then, the air compressor electrical power consumption ($P_{compressor}$) is evaluated using (5):

$$P_{compressor}(\dot{m}_{air}, T_{amb}, p_{ratio}) = \frac{\dot{m}_{air} \cdot c_{p,air}(T_{amb}) \cdot T_{amb} \cdot p_{ratio}^{\frac{k-1}{k}} - 1}{\eta_{elec} \cdot \eta_{adiabatic}(\dot{m}_{air}, p_{ratio})} \quad (5)$$

where $c_{p,air}$ and k stand for the air specific heat as a function of the ambient temperature T_{amb}, and the specific heat ratio for the air, respectively. η_{elec} is the compressor motor drive electrical efficiency which is assumed having a constant value here.

When it comes to the radiator, two one-dimensional lookup tables are considered that map the heat transfer coefficient between coolant and external air (h_{rad}) as a function of the

vehicle speed ($speed_{veh}$) for the radiator fan being activated or de-activated, respectively, Kroger (1984). The radiator fan state is considered in the binary variable $state_{fan}$. Then, the temperature of the coolant at the radiator outlet ($T_{coolant,out}$) can be calculated as follows:

$$T_{coolant,out} = T_{coolant,in} - 0.5 \cdot \frac{A_{rad} \cdot h_{rad}(speed_{veh}, state_{fan}) \cdot (T_{coolant,in} - T_{amb})}{\dot{m}_{coolant} \cdot c_{p,coolant}} \quad (6)$$

where $T_{coolant,in}$ is the coolant temperature at the radiator inlet and equals the value of $T_{coolant,out}$ in the previous time instant. $\dot{m}_{coolant}$ is the coolant mass flow rate through the coolant pump, while $c_{p,coolant}$ is the specific heat of the coolant. A_{rad} stands for the radiator frontal area, while the 0.5 constant in (6) accounts for the numerical model being initially calibrated for a 0.5 m² radiator. When activated, the radiator fan is assumed here constantly consuming a 300 watts electrical power ($P_{radiator-fan}$).

Coolant is circulated through the fuel cell system thanks to the coolant pump, which moves energy through the stack, humidifier, and radiator. The instantaneous heat removed by the coolant ($Q_{coolant}$) can be calculated using (7):

$$Q_{coolant} = \dot{m}_{coolant} \cdot c_{p,coolant} \cdot \left(T_{stack} - T_{coolant,out}\right) \quad (7)$$

From an electrical point of view, the parasitic power consumed by the coolant pump ($P_{coolant-pump}$) can be obtained by interpolating in a one-dimensional lookup table as a function of $\dot{m}_{coolant}$.

The stack temperature in the next time instant ($T_{stack,next}$) can be determined according to the thermal balance reported in (8):

$$\begin{aligned}
T_{stack,next} &= T_{stack} \\
&+ \left(Q_{stack} - Q_{coolant} - Q_{ambient} - Q_{air} - Q_{water-vapor} \right. \\
&\left. + Q_{condenser}\right) \cdot \frac{\Delta t}{L_{lumped}}
\end{aligned} \quad (8)$$

with

$$Q_{ambient} = h_{stack} \cdot (T_{stack} - T_{amb})$$
$$Q_{air} = \dot{m}_{air} \cdot c_{p,air} \cdot \left(T_{air,in} - T_{stack}\right)$$
$$Q_{water-vapor} = \dot{m}_{wv-in} \cdot c_{p,wv}\left(T_{wv,in}\right) - \dot{m}_{wv-out} \cdot c_{p,wv}(T_{stack})$$
$$Q_{condenser} = \dot{m}_{H20,condensed} \cdot h_{fg}$$

where Δt and L_{lumped} are the simulation time step in seconds and the lumped stack thermal capacitance in joules per kelvin, respectively. $Q_{ambient}$ is the overall heat transferred from the stack to the ambient by means of natural convection. In this term, h_{stack} is the overall heat transfer coefficient associated with natural convection. Q_{air} is the heat contribution brought by the air provided by the compressor at temperature $T_{air,in}$. $Q_{water-vapor}$ accounts for the enthalpy variation of water and vapor between inlet and outlet of the stack. In this term, $\dot{m}_{wv-in}$ and $\dot{m}_{wv-out}$ are the mass flow rates of water and vapor entering and exiting the stack, respectively. $c_{p,wv}$ is the corresponding specific heat for water and vapor which is evaluated for temperatures $T_{wv,in}$ and T_{stack}, respectively. $Q_{condenser}$ is the heat exchanged between stack and condenser,

which can be evaluated considering the mass flow rate of the condensed water ($\dot{m}_{H2O,condensed}$) and the heat of vaporization of water (h_{fg}).

2.4 Net system power

The last step of the implemented fuel cell system modelling approach involves determining the net electrical power provided by the system. This is achieved by performing an electrical power balance subtracting the overall auxiliary losses from the system gross power as reported in (9):

$$P_{stack-net} = P_{stack-gross} - P_{compressor} - P_{coolant-pump} - P_{radiator-fan} - P_{condenser-fan} \quad (9)$$

where $P_{condenser-fan}$ is the power consumption of the condenser fan, which is assumed here being 300 watts when the fuel cell system is in operation.

Finally, the value of $P_{stack-net}$ is compared with the net power request evaluated in sub-section 2.1. In case of a mismatch, a solver is implemented to iteratively adjust the value of stack current density until comparable values are obtained between the power requested and the power provided.

3. PREDICTIVE CONTROL FRAMEWORK

This section describes the implemented predictive control framework for thermal management of the automotive fuel cell system. In this work, the implemented predictive control algorithm relies on DP. DP is one of the most common approaches to evaluate the global optimal solution for a given dynamic control problem, Kolodziejak et al. (2019). DP requires a priori knowledge of the entire time horizon of the considered control problem, i.e. the entire driving mission in terms of vehicle speed and fuel cell system power request over time in this case. Discretized arrays for control variables and state variables need definition in DP. Control variables are directly managed by the control system under consideration. On their behalf, state variables characterize by their values being tracked and updated throughout the driving mission under analysis. The control variable set U and the state variable set X for the fuel cell system thermal control problem under investigation are illustrated in (10):

$$U = \left\{ \begin{array}{c} \frac{P_{stack-gross}}{P_{stack-request}} \\ state_{fan} \\ \dot{m}_{coolant} \\ \dot{m}_{air} \end{array} \right\} \quad ; \quad X = \left\{ \begin{array}{c} T_{stack} \\ T_{coolant} \end{array} \right\} \quad (10)$$

The implemented DP version involves controlling the ratio between fuel cell system gross power and the corresponding net power request, along with the radiator fan state, the coolant mass flow rate provided by the pump, and the air mass flow rate provided by the compressor. On the other hand, X includes the temperature values for both the stack and the coolant. In this way, stack and coolant temperatures can appropriately be updated at each time instant throughout the driving mission according to (8) and (6), respectively.

Once U and X are defined, DP exhaustively explores all the possible combinations of discretized values of control and

state variables backwardly from the last time instant (t_{end}) of the driving mission to the initial one (t_0) while identifying the control trajectories that minimize the overall value of a predefined cost functional J. Optimization constraints are considered in this process. Both J and constraints retained in this work are reported in (11).

$$J = \int_{t_0}^{t_{end}} \dot{m}_{H2}(t)dt$$

Subject to:

$$T_{stack} \leq T_{stack-lim}$$
$$P_{stack-net} \geq P_{stack-request}$$
$$state_{fan}(speed_{veh} = 0) = 0 \quad (11)$$
$$\dot{m}_{coolant}(speed_{veh} = 0) = 0$$
$$\dot{m}_{air}(speed_{veh} = 0) = 0$$
$$\dot{m}_{coolant-min} \leq \dot{m}_{coolant} \leq \dot{m}_{coolant-MAX}$$
$$\dot{m}_{air-min} \leq \dot{m}_{air} \leq \dot{m}_{air-MAX}$$

Here, the optimal control problem involves minimizing the hydrogen consumption in the overall driving mission. The value of stack temperature is prevented to exceed the operational limit $T_{stack-lim}$ which is assumed being 95° C here. The net power provided by the fuel cell system needs to always be equal or higher than the corresponding power request coming from the FCEV control logic. The thermal system of the fuel cell (i.e. radiator fan, coolant pump and compressor in this case) is prevented from being activated if the vehicle is not in motion in order not to potentially undermine passenger acoustic comfort. Finally, values of both the coolant mass flow rate and the air mass flow rate are constrained within the physical operational limits of the coolant pump and the compressor, respectively. In this framework, subscripts 'min' and 'MAX' respectively denote lower and upper operational boundaries. The open-source 'DynaProg' DP function is used in this work for solving the illustrated optimal control problem for thermal management of automotive fuel cell systems., Miretti et al. (2021).

4. SIMULATION RESULTS AT HIGH AMBIENT TEMPERATURES

In this section, numerical results are presented for the illustrated predictive control approach for thermal management of automotive fuel cell systems at high ambient temperatures. High ambient temperatures represent a noteworthy case study since they notably accelerate the fuel cell degradation mechanisms, Salam et al. (2020). Data considered in this work for a representative fuel cell electrified passenger car are reported in Table 1 and have been retained from Advisor™. The ambient temperature as well as the initial value for T_{stack} and $T_{coolant}$ have been set to 30° C to account for hot climate conditions. Table 2 shows the retained discretization grids for both control and state variables, where the number of elements for each variable has been decided aiming at the right trade-off between discretization accuracy and overall computational cost for running DP. 2,940 and 5,041 elements are considered in total for the control variables and the state variables, respectively, which brings the total number of possible control actions operable by DP at each

Table 1. Representative FCEV parameters.

Component	Parameter	Value
Vehicle	Mass	1500 kg
	Frontal area	2.0 m^2
	Drag coefficient	0.335
	Tyre radius	0.282 m
Electric motor	Maximum power	75 kW
Transmission	Direct drive ratio	6.67
Battery pack	Nominal voltage	292 V
	Capacity	7.4 Ah
Fuel cell system	Maximum power	55 kW
	Cell area	678 cm^2
	Number of cells	210
	Max cell voltage	0.94 V

Table 2. Discretizing control and state variables in DP.

Type	Variable	Discretization	Units of measure
Control variables	$\dfrac{P_{stack-gross}}{P_{stack-request}}$	(1:0.02:1.4)	[-]
	$state_{fan}$	[0 1]	[-]
	$\dot{m}_{coolant}$	[0 0.05 0.1 0.15 0.2 0.3 0.4 0.5 1 1.5]	kg/s
	$\dot{m}_{air}$	(64.2:117.7:770.4)	g/s
State variables	T_{stack}	(30:1:100)	°C
	$T_{coolant}$	(30:1:100)	°C

discretized time instant in the drive cycle up to 14,820,540. Here, the drive cycle is discretized with 1 second steps.

The FCEV is simulated performing the Worldwide Harmonized Light Vehicle Test Procedure (WLTP) which involves a 30-minute 23.4 km drive cycle. Eight different DP simulations are performed here considering one (WLTPx1) to eight (WLTPx8) steady repetitions of WLTP. Once the control trajectories over time are generated by DP for the entire driving mission, these are fed to a forward model of the fuel cell system to evaluate the time series of stack and coolant temperatures along with overall energy consumption values in the driving mission. This allows evaluating energy and thermal balances while avoiding the dependence of the DP simulation results on the discretization of state variables. Figure 2 shows time series of stack temperature as evaluated in the fuel cell system forward model considering the control trajectories provided by DP over different numbers of WLTP repetitions. On the other hand, Table 3 reports energy statistics for each simulation case considering one to eight WLTP repetitions at 30° C ambient temperature.

Looking at Fig. 2, in each considered simulation case DP allows the stack temperature arising above 80°C, and then controls it to swing in a window comprised between 80° C and 95° C (i.e. the maximum allowed value). A possible explanation for this optimal control behaviour predicted by DP in this case can be provided looking at the fuel cell system efficiency map displayed in Fig. 3 as a function of the current
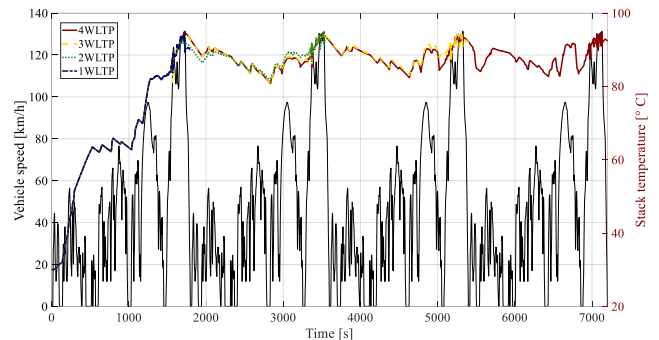

Fig. 2. Time series of stack temperature as predicted by the DP based predictive fuel cell thermal management strategy over one to four WLTP repetitions.

density request and the stack temperature. Indeed, as the stack temperature increases, the fuel cell system can operate at higher efficiency values even at higher values of current density request. As shown in Fig. 3, the implemented DP based predictive control framework thus allows the fuel cell system operating points to locate in high efficiency areas for both WLTPx1, WLTPx4 and WLTPx8 simulation cases. In detail, the fuel cell stack efficiency varies from 55% to 75% for almost the entire totality of working points. Indeed, the average stack efficiency values reported in Table 3 corroborate this observation for the remaining simulation cases as well. Moreover, as the length of the driving mission increases, the average stack efficiency gradually increases from 62.5% to 63.0%. This can be explained by the fuel cell system operation at higher stack temperatures being preserved longer in the

Table 3. Energy statistics for the automotive fuel cell system simulated being thermally controlled by DP over different numbers of WLTP repetitions.

|		WLTP x1	WLTP x2	WLTP x3	WLTP x4	WLTP x5	WLTP x6	WLTP x7	WLTP x8
Energy loss [kJ]	Air compressor energy	3,395	8,542	14,564	20,017	25,398	30,915	36,467	42,030
	Coolant pump energy	88	134	194	300	420	543	667	791
	Radiator energy	18	43	74	108	145	180	215	250
	Condenser fan energy	328	656	985	1313	1641	1969	2297	2626
	Chemical loss	11,141	23,016	35,548	47,633	59,677	71,776	83,910	96,037
Statistics	Net energy generation [kJ]	14,745	29,489	44,234	58,978	73,723	88,467	103,212	117,957
	Gross energy generation [kJ]	18,573	38,863	60,050	80,716	101,328	122,075	142,859	163,653
	Average stack efficiency [%]	62.5	62.8	62.8	62.9	62.9	63.0	63.0	63.0
	Average FC system efficiency [%]	49.6	47.7	46.3	46.0	45.8	45.6	45.5	45.4
	H2 consumption [kg]	0.25	0.52	0.80	1.07	1.34	1.62	1.89	2.16
	Driving mission length [km]	23.4	46.8	70.2	93.6	117.0	140.4	163.8	187.2
	Predicted H2 economy [kg/100 km]	1.06	1.10	1.13	1.14	1.15	1.15	1.15	1.16
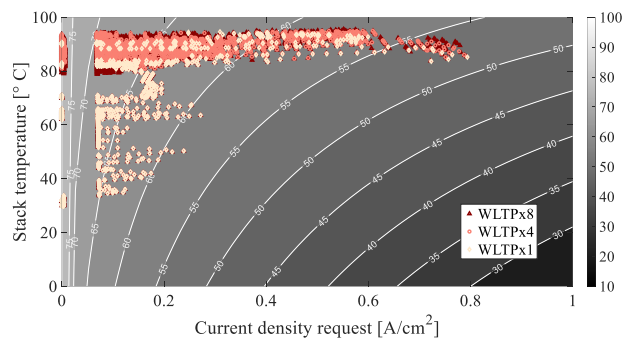
Fig. 3. Efficiency map and operating points of the automotive fuel cell system thermally controlled by DP in WLTPx1, WLTPx4 and WLTPx8 drive cycles.

driving mission once the initial warmup has been completed. Nevertheless, an opposite trend can be observed in Table 3 for the fuel cell system efficiency that decreases as the length of the driving mission increases. This relates to the progressively higher amount of energy per kilometer that the auxiliaries consume to cool down the stack. For example, looking at the compressor energy in Table 3, 224.5kJ compressor energy per kilometer is required by the predictive DP controller in WLTPx8. On the other hand, for a driving mission involving a single WLTP, the required compressor energy amounts to 145.1kJ per kilometer only.

As reported in Table 3, the implemented DP based predictive control approach for thermal management of automotive fuel cell systems overall entails a greater use of the air compressor among the auxiliary devices. On the other hand, the coolant pump and the radiator are controlled to operate less which allows saving energy. Thanks to the implemented predictive controller, the forecasted H2 economy value remains quite constant even when higher driving distances are covered (e.g. 100km to 190km).

5. CONCLUSIONS

This paper presents a predictive control framework for thermal management of automotive fuel cell system. Particularly, the study focuses on the optimization of the fuel cell system performance at high ambient temperature.

The electrochemical and thermal models of a fuel cell system for automotive applications is considered. Then, DP is implemented as global optimal predictive thermal management approach. The control variables involve the gross stack power, the radiator fan state, along with coolant and air mass flow rates circulating in the coolant pump and the air compressor, respectively.

Simulation results for different numbers of WLTP repetitions at high ambient temperatures demonstrate that high fuel cell stack average efficiency can be preserved (i.e. 62.5% to 63.0%). This is related to an increase of the fuel cell stack working temperature which allows the fuel cell stack to operate at higher efficiency. Moreover, thanks to the predictive controller, the forecasted H2 economy value stays rather constant even when longer driving distances are performed that require higher cooling energy by the auxiliaries.

Further studies in this area may include developing real-time predictive thermal management systems for FCEVs. The provided DP off-line approach may be used to generate the ideal benchmark and off-line optimized training data in this context.

REFERENCES

Ajanovic, A., & Haas, R. (2019). Economic and environmental prospects for battery electric-and fuel cell vehicles: a review. Fuel Cells, 19(5), 515-529.

Bethoux, O. (2020). Hydrogen Fuel Cell Road Vehicles: State of the Art and Perspectives. Energies, 13(21), 5843.

Binrui, W., Yinglian, J., Hong, X., & Ling, W. (2009, June). Temperature control of PEM fuel cell stack application on robot using fuzzy incremental PID. In 2009 Chinese Control and Decision Conference (pp. 3293-3297). IEEE.

Gurski, S.D. (2002) "Cold-start effects on performance and efficiency for vehicle fuel cell systems", M. Sc. thesis, Virginia Tech.

Han, J., Yu, S., & Yi, S. (2017). Advanced thermal management of automotive fuel cells using a model reference adaptive control algorithm. International journal of hydrogen energy, 42(7), 4328-4341.

Ibrahim, B. K., Aziah, M. A. N., Ahmad, S., Akmeliawati, R., Nizam, H. M. I., Muthalif, A. G. A., ... & Hassan, M. K. (2012). Fuzzy-based temperature and humidity control for HV AC of electric vehicle. Procedia Engineering, 41, 904-910.

Kolodziejak, D. P. H., Pham, T. H., Hofman, T., and Wilkins, S. (2019) "An optimization and analysis framework for TCO minimization of plug-in hybrid heavy-duty electric vehicles", IFAC-PapersOnLine, 52(5), 484-491.

Kröger, D. G. (1984) "Radiator Characterization and Optimization." SAE Transactions, vol. 93, pp. 984–90.

Larminie, J., Dicks, A., and McDonald, M. S. (2003) "Fuel cell systems explained", Chichester, UK: J. Wiley.

Liu, J., Zhou, H., Zhou, X., Cao, Y., & Zhao, H. (2011, August). Automotive air conditioning system control—A survey. In Proceedings of 2011 International Conference on Electronic & Mechanical Engineering and Information Technology (Vol. 7, pp. 3408-3412). IEEE.

Markel, T., Brooker, A., Hendricks, T., Johnson, V., Kelly, B., Kramer, B. et al. (2002) "ADVISOR: a systems analysis tool for advanced vehicle modeling", Journal of power sources, vol. 110, no. 2, pp. 255-266.

Miretti, F., Misul, D., and Spessa, E. (2021). "DynaProg: Deterministic Dynamic Programming solver for finite horizon multi-stage decision problems", SoftwareX, 14, 100690.

Salam, M. A., Habib, M. S., Arefin, P., Ahmed, K., Uddin, M. S., Hossain, T., & Papri, N. (2020). Effect of temperature on the performance factors and durability of proton exchange membrane of hydrogen fuel cell: A narrative review. Mater. Sci. Res. Indian, 2, 91-179.

Xie, Y., Liu, Z., Liu, J., Li, K., Zhang, Y., Wu, C., ... & Wang, X. (2020). A Self-learning intelligent passenger vehicle comfort cooling system control strategy. Applied Thermal Engineering, 166, 114646.

Zhang, B., Lin, F., Zhang, C., Liao, R., & Wang, Y. X. (2020). Design and implementation of model predictive control for an open-cathode fuel cell thermal management system. Renewable Energy, 154, 1014-1024.